Prediction of Non-Linear Pile Foundation Response to Vertical Vibration

Toyoaki Nogami
University of Cincinnati, Cincinnati, Ohio

Hsiao-Lian Chen
M.W. Kellog Company, Houston, Texas

Recommended Citation

Prediction of Non-Linear Pile Foundation Response to Vertical Vibration

Paper No. 5.39

Toyoaki Nogami
Professor of Civil Engineering, University of Cincinnati, Cincinnati, Ohio

Hsiao-Lian Chen
Senior Engineer, M.W. Kellog Company, Houston, Texas

SYNOPSIS A rational and yet convenient approach is presented to account for the dynamic soil-pile interaction in the vertical vibration analysis of a nonlinear pile foundation. Once elastic soil properties and static complex unit load transfer curves are provided, the approach is capable of reproducing the dynamic and nonlinear conditions mutually coupled. The concept of the approach is verified by numerical analyses. The proposed approach is demonstrated for the prediction of vibration response of a selected pile foundation in the field. Both static load tests and vibration tests were conducted previously on this pile foundation. Inputs for the analysis are obtained from the previous static test results. The comparison of the predicted responses with those observed indicates that the proposed approach appears to be reasonable.

INTRODUCTION

Various methods have been developed to compute the dynamic response of pile foundations. Among them, those simplifying soil with a Winkler model are most convenient and practical for computation. However, a soil medium is continuous and therefore a great difficulty arises in defining the parameters of this model. In the static condition, such a treatment of a continuous medium is totally illogical therefore the model parameters are defined empirically, simply to fit the target response. In the dynamic condition, however, it is logical from the wave propagation mechanism point of view (Nogami and Novak, 1980) and thus the model parameters can be defined from the logical treatment.

Traditionally, nonlinear pile response is analyzed by using a Winkler model defined by a unit load transfer curve such as so-called p~y and t~z curves (e.g. Matlock, 1970). For the linear elastic or visco-elastic condition, Novak (1974) defined the parameter of a dynamic Winkler soil-pile interaction model, which can produce the pile responses amazingly close to those computed by using a three-dimensional continuous model (Sanchez Salinero, 1982). Rational reasoning for Novak's definition of model parameters is provided in view of the mechanism of wave propagation (Nogami and Novak, 1980). Combining the traditional approach with the above rational approach for a linear elastic model, the first author has proposed nonlinear dynamic soil-pile interaction models both for the time-domain and frequency-domain (e.g. Nogami and Konagai, 1986, Nogami et al., 1992). This paper deals with a frequency domain model for the vertical response.

SOIL-PILE INTERACTION FORCE

Soil around the pile shaft is divided into the near field and far field. The near field represents the soil in the close vicinity of the pile shaft, where strong nonlinearity is induced by large pile shaft displacement. The far field represents the soil outside the near field soil. The soil in this region is assumed to be located at a distance from the pile far enough to behave more or less elastically even if the shaft displacement is large. The energy exerted on soil by pile motion must pass through the near field before reaching the far field. The

nonlinearity in the near field interferes this energy transmission to the far field, resulting in coupling between the dynamic condition and nonlinear condition. This coupling can be reproduced rationally by a subgrade model in which the near field model (near field element) is connected to the far field model (far field eleme.it) in series as shown in Fig. 1.
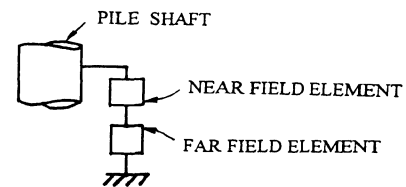

Fig. 1 Soil-pile interaction model made of near field and far field elements

For the steady state cyclic environment, the relationship between the pile shaft displacement and soil reaction force at a given depth draws a hysteresis loop during one cycle of motion as shown in Fig. 2. The maximum values of force and displacement are amplitudes. The enclosed area is related with damping defined herein through the relation

$$D = \frac{1}{2\pi} \frac{AREA}{p_{max} w_{max}} \tag{1}$$

where AREA = enclosed area in the loop; p_{max} and w_{max} = force and displacement amplitudes, respectively; and D = damping factor. The force amplitude and damping in a hysteresis loop are dependent on displacement amplitude and frequency. The soil stiffness for a hysteresis behavior is conveniently defined in the frequency domain by a complex number such that

$$Real \ k = \frac{p_{max}}{w_{max}} \quad and \quad Imag. \ k = \frac{2D \, p_{max}}{w_{max}} \tag{2}$$
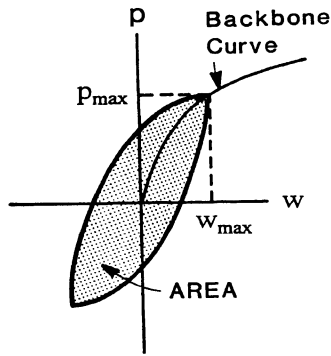
p **Backbone Curve**

Fig. 2 Hysteresis loop in cyclic motion

Therefore, if two curves as shown in Fig. 3 are available, the complex soil stiffness can be obtained as secant slopes of these curves. A set of these curves is called herein a complex unit load transfer curve (CULT curve), in which the real and imaginary parts define respectively the real and imaginary parts of the stiffness. The CULT curve is dependent on frequency and its real part is a backbone curve of hysteresis loops at various displacement amplitudes. In a conventional cyclic response analysis with a Winkler subgrade model, so called cyclic unit load transfer curves are provided as inputs. These are the real parts of the static CULT curves. In the present approach, both the real and imaginary parts of the static CULT curve are assumed to be provided as input information.
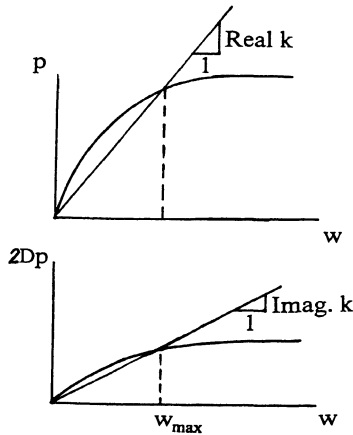

Fig. 3 Complex unit load transfer curve made of real and imag. parts

(a) Far Field Element

The far field element is modeled as a complex spring to reproduce the linear elastic behavior of a far field at the outer edge of a near field of size R. Its stiffness is, therefore, assumed to be defined from the vertical vibration of a rigid massless circular cylinder with a radius R, vertically embedded in an infinite medium. The stiffness for such conditions was formulated previously as (Novak et al., 1978)

$$k_f(\omega) = 2\pi G^* \cdot \frac{a_R^* K_1(a_R^*)}{K_0(a_R^*)} \qquad (3)$$

where k_f = stiffness of the far field element; $a_R^* = R\omega / v_s^*$; $v_s^* = \sqrt{G^* / \rho}$; $G^* = G(1+i2D)$; G, D and ρ = shear modulus, damping factor and unit mass of soil, respectively; R = radius of the cylinder; and ω = circular frequency. Eq. 3 fails to produce a reasonable value for the frequencies lower than the fundamental frequency of ground and thus the stiffness computed by Eq. 3 is modifies as shown in Fig. 4. The static k_f, $k_f(0)$, in Fig, 4 is yet to be defined.
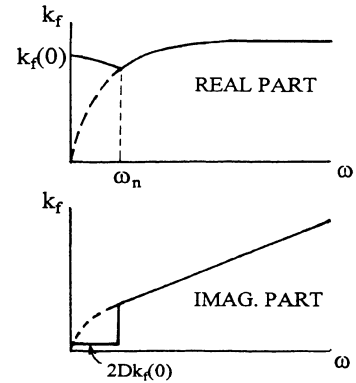

Fig. 4 Corrections in variation of stiffness with frequency

A pile of a radius r_0 is assumed to be subjected to a static axial load. Pile displacement at a given depth, w, can be written as

$$w = w_R + \Delta w_{r_0,R} \qquad (4)$$

where w_R = soil displacement at a radial distance R; $\Delta w_{r_0,R}$ = difference between the soil displacements at R and r_0. In the static condition, the integration of the vertical shear stress around the circle of a radius R, p_R, is equal to the soil reaction force at the soil-pile interface p. Therefore, dividing Eq. 4 by the soil reaction force, p, and using a continuum solution for the second term, Eq. 4 is rewritten as

$$\frac{1}{k(0)} = \frac{1}{k_f(0)} + \left(\frac{1}{2\pi G} \log_e \frac{R}{r_0} \right)$$

or

$$k_f(0) = \left[\frac{1}{k(0)} - \left(\frac{1}{2\pi G} \log_e \frac{R}{r_0} \right) \right]^{-1} \qquad (5)$$

where $p/w = k(0)$; $p/w_R = p_R/w_R = k_f(0)$; and $\Delta w_{r_0,R}/p = \log_e(R/r_0)/(2\pi G)$, formulated for an infinitely long rigid cylinder with radius r_0, vertically embedded in an infinite medium. k(0) is the elastic stiffness defined by the initial secant slope in the real part of input static CULT curve.

With k_f given by either Eq. 3 or 5, the dynamic force-displacement relationship of the far field is expressed as

$$p_R = k_f(\omega) w_R \qquad (6)$$

where p_R = the resultant force of the integration of the vertical shear stress around the circle of a radius R.

402

(b) Near Field Element

A near field element represents the soil in the close vicinity of a pile, where a strong nonlinearity is induced. This element consists of a frequency independent nonlinear complex spring and a consistent mass. The latter is for taking into account the dynamic condition in a near field. In the static condition, the stiffnesses of near field and far field elements (k_n and $k_f(0)$, respectively) and the stiffness of a subgrade model made of these elements ($k(0)$) are related through

$$\frac{1}{k(0)} = \frac{1}{k_n} + \frac{1}{k_f(0)}$$

or

$$k_n = \frac{k_f(0)k(0)}{k_f(0) - k(0)} \tag{7}$$

$k_f(0)$ is previously given by Eq. 5, and $k(0)$ is defined by the secant slope in the input static CULT curve at an appropriate displacement amplitude.

Assuming a linear variation of soil displacement with a radial distance from the pile, a consistent mass matrix at r_0 and R is expressed as

$$\begin{bmatrix} m_{r_0} & m_{r_0 R} \\ m_{r_0 R} & m_R \end{bmatrix} = \frac{\pi \rho r_0^2}{6} (R/r_0 - 1) \begin{bmatrix} R/r_0 + 3 & 3R/r_0 + 1 \\ 3R/r_0 + 1 & R/r_0 + 1 \end{bmatrix} \tag{8}$$

With k_n given in Eq. 7 and a consistent mass given in Eq. 8, the dynamic force-displacement relationship of the near field element is expressed as

$$\begin{Bmatrix} p_{r_0} \\ p_R \end{Bmatrix} = \left[k_n \begin{bmatrix} 1 & -1 \\ -1 & 1 \end{bmatrix} - \omega^2 \begin{bmatrix} m_{r_0} & m_{r_0 R} \\ m_{r_0 R} & m_R \end{bmatrix} \right] \begin{Bmatrix} w_{r_0} \\ w_R \end{Bmatrix} \tag{9}$$

(c) Soil-Pile Interaction Force and Pile Response

Combining Eqs. 6 and 9, the following expression is obtained:

$$\begin{Bmatrix} p_{r_0} \\ p_R \end{Bmatrix} = \left[\begin{bmatrix} k_n & -k_n \\ -k_n & k_n + k_f(\omega) \end{bmatrix} - \omega^2 \begin{bmatrix} m_{r_0} & m_{r_0 R} \\ m_{r_0 R} & m_R \end{bmatrix} \right] \begin{Bmatrix} w_{r_0} \\ w_R \end{Bmatrix} \tag{10}$$

External force acting on the interaction model is the soil-pile interaction force, p, only (i.e. $p_{r_0} = p$ and $p_R = 0$) and w_{r_0} is equal to the pile shaft displacement (i.e. $w_{r_0} = w$). Solving Eq. 10 for w_{r_0} with these conditions, the soil-pile interaction force is expressed as

$$p = k(\omega)w \tag{11}$$

where

$$k(\omega) = k_n - \omega^2 m_{r_0} - \frac{k_n^2 + 2\omega^2 k_n m_{r_0 R} + \omega^4 m_{r_0 R}^2}{k_n + k_f(\omega) - \omega^2 m_R} \tag{12}$$

Therefore, if a CULT curve is provided for the static condition, the dynamic soil stiffness, $k(\omega)$, can be completely defined at any frequency at any displacement amplitude.

Vertical vibration of a pile foundation is governed by

$$-E_p A \frac{d^2 w}{dz^2} - \omega^2 m_p w = -p \tag{13}$$

where E_p, m_p and A = Young' modulus, mass per unit length and cross section area of pile, respectively. Solving Eq. 13 with Eq. 11 for given boundary conditions of the pile shaft, the dynamic response of a pile foundation is formulated. In the development of formulation, the pile shaft is divided into a number of segments and the values of soil properties and stiffness, $k(\omega)$, are assumed to be uniform within an individual segment. Since k_n is dependent on the displacement amplitude which in turn is dependent on k_n, an iteration scheme is used to find the values of k_n and displacement mutually compatible.

VERIFICATION OF CONCEPT

An important feature of the present approach is that, if a CULT curve is provided only for the static condition, the dynamic nonlinear soil stiffness can be determined with the approach above explained. Its main concept is verified by using the finite element method (FEM) and the finite-boundary element method (FEM-BEM). The conditions considered for the verification are an infinitely long rigid circular cylinder which is vertically embedded in an infinite nonlinear medium.

First, the CULT curve is constructed for the static cyclic condition by using the finite element method. The stress-strain and damping-strain relations used are those proposed by Hardin and Dreinovich (1972). They are

$$G = \frac{G_{max}}{\gamma/\gamma_r} \quad \text{and} \quad D = \frac{D_{max}\,\gamma/\gamma_r}{1 + \gamma/\gamma_r} \tag{14}$$

where G and D = strain dependent shear modulus and damping of soil, respectively; G_{max} and D_{max} = maximum values of G and D, respectively; and $\gamma_r = \tau_{max}/G_{max}$ with $\tau_{max} = c + \sigma'\tan\phi$ and σ' = effective normal stress. G_{max}, D_{max}, and τ_{max} are defined for typical soil conditions at a depth 7 feet below the ground surface at the UH pile load test site (i.e. $G_{max} = 24.37$ ksi; $D_{max} = 0.3$; OCR = 10; $K_0 = 2$; c = 0.4 ksf; $\phi = 26°$). The fixed boundary condition is assumed at a radial distance $50r_0$. Given a displacement amplitude with a real number at the cylinder, the static complex interaction force is computed. This procedure is repeated for various displacement amplitudes to construct a CULT curve.

Using the above obtained CULT curve as input, variations of the dynamic soil stiffness with displacement amplitude are computed at frequencies a_0 (= $r_0\omega/v_s$) = 0.01 and 0.1 by using Eq. 12. Sizes R used in the analyses are $1.5r_0$, $2r_0$ and $3r_0$. They are also computed by the FEM-BEM, in which the BEM is applied at the outer edge of the finite element mesh area to reproduce the behavior of a medium laterally extending to infinity. This FEM-BEM method can directly simulate the behavior affected by both the nonlinear and dynamic conditions simultaneously. The computed results by these two methods are compared in Fig. 5. The figure indicates that the stiffness computed by the present method is very little affected by the difference in size R. It is seen that the present approach can reproduce very well the dynamic behavior in the nonlinear environment or nonlinear behavior in the dynamic environment.

PREDICTION OF VIBRATION RESPONSE

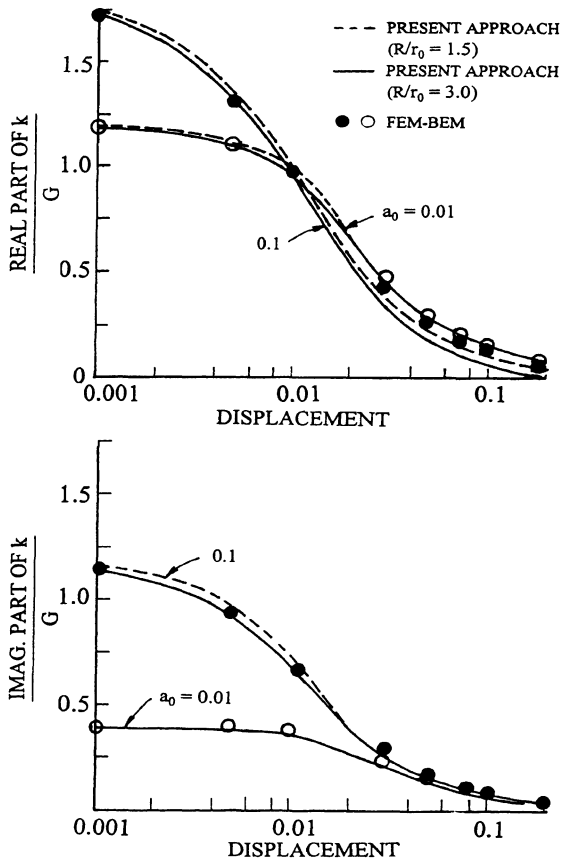Both static monotonic load tests and vibration tests were

Fig. 5 Nonlinear dynamic soil stiffnesses
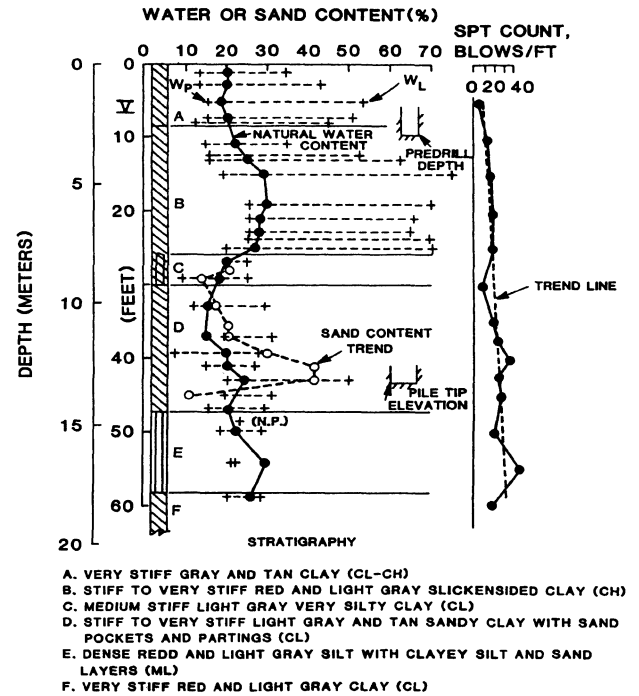computed by proposed approach and FEM-BEM

Fig. 6 Stratigraphy of soil at test site

A. VERY STIFF GRAY AND TAN CLAY (CL-CH)
B. STIFF TO VERY STIFF RED AND LIGHT GRAY SLICKENSIDED CLAY (CH)
C. MEDIUM STIFF LIGHT GRAY VERY SILTY CLAY (CL)
D. STIFF TO VERY STIFF LIGHT GRAY AND TAN SANDY CLAY WITH SAND POCKETS AND PARTINGS (CL)
E. DENSE REDD AND LIGHT GRAY SILT WITH CLAYEY SILT AND SAND LAYERS (ML)
F. VERY STIFF RED AND LIGHT GRAY CLAY (CL)

Fig. 7 Distribution of undrained shear strength of soil at test site

conducted on a common pile at the UH site (O'Neill et al., 1981). The input CULT curves are obtained from the static tests. With these curves, the responses of the pile during the vibration test are predicted by the present approach. The predicted responses are compared with the observed responses in the field.

(a) Site and Test Conditions

Detailed properties and characterization of the test site soil are described by O'Neill et al. (1981). Figs. 6, 7 and 8 are reproduced from this reference to show the stratigraphy, undrained shear strength and Young's modulus of soil at the test site, respectively. In general, the soil is very stiff, saturated clay preconsolidated by desiccation in the order of 6 tsf. The water table at the site is located at a depth 7.5 ft, below the ground surface. The layers depicted in Fig. 6 become generally less plastic, less compressible, and sandier with depth. Stratum C is silty and presents a zone of weathering on the prehistoric surface of a Pleistocene terrace. Soils above this stratum are slickensided, and those below that depth contain numerous sand seams.

A set up of pile vibration test is shown in Fig. 9. The pile is a closed end steel tubular pile of 20.75 in. O.D. with a 0.365 inch thick wall. It was driven to a penetration depth 43 ft. and tested statically to failure in compression before the vibration test. Following the static tests and before the dynamic tests, the pile was redriven to a final penetration of 44 ft. in order to establish the conditions at the soil-pile interface that would have existed before the static tests. A rigid cap
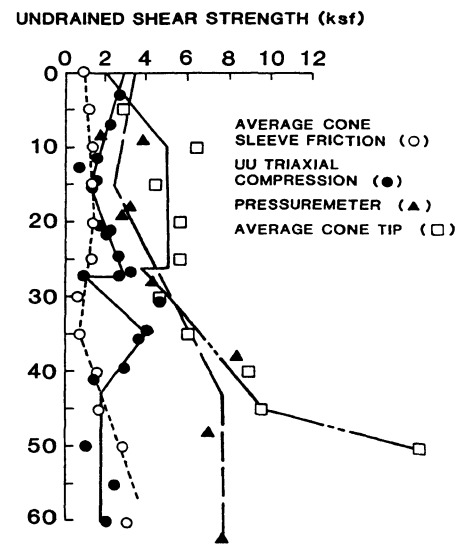
mass, weighed 13,825 lb., was attached to the pile top. Strain gages were attached on the interior of the pile wall at intervals of 5 ft. from the base of the cap to the pile tip. In addition, the pile and cap-mass were instrumented with accelerometers and geophones. A linear inertia-mass vibrator, weighed 11,075 lb., was mounted on the cap-mass. Load cells were placed between the vibrator and the cap-mass.

Frequency downsweep load was applied from 50 Hz to 5 Hz during 30 sec. The load amplitude was held constant during each sweep at a level of 400, 4000 or 8000 lb.
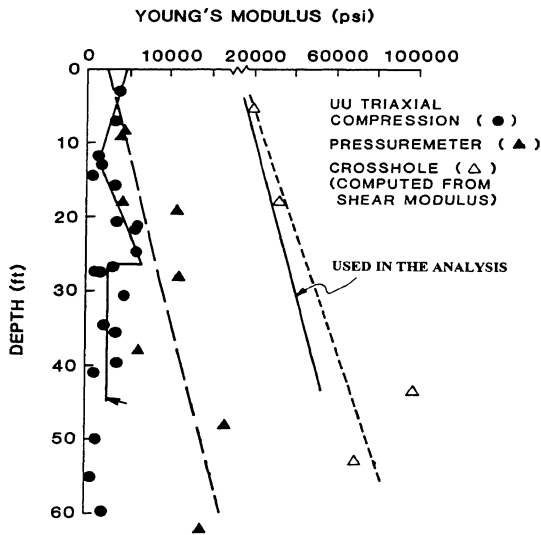

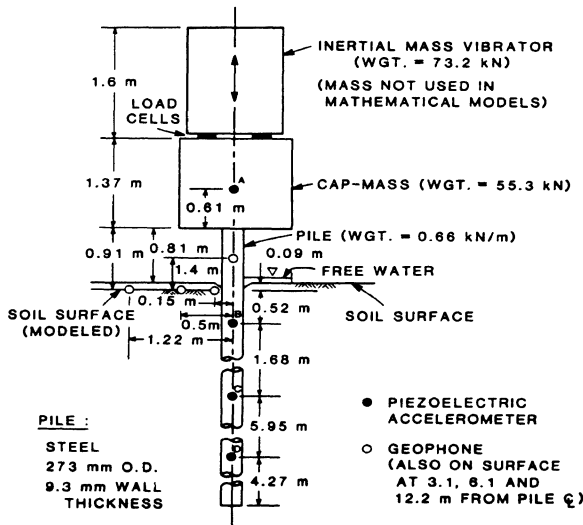Fig. 8 Distribution of Young's modulus of soil at test site

Fig. 9 Test pile and instrumentation system

(b) Inputs for the Analysis

The elastic (visco-elastic) parameters of soil are shear modulus (G), Poisson's ratio(v) and damping factor (D). Poisson's ration 0.5 was assumed. The distribution of Young's modulus with depth varies widely depending on a test method as shown in Fig. 8. The previous investigation on pile groups at the site (Nogami and Paulson, 1984) found the proper distribution as indicated in the figure. The damping factor, D, in the far field is that corresponding to small strain levels. Resonant column tests results indicate these values at depths 6.6, 16.7

and 31.7 ft to be in the range of 2~5 % (Blaney and O'Neill, 1986). A uniform value of 2% is assumed along the depth.

Unit load transfer curves of the pile considered herein were defined in the previous study on the static response (Nogami and Paulson, 1984). They were generated from a formulation proposed by Vijayvergiya (1977) but with some modification. This modified formulation is

$$ p = p_{max} \left[2\left(\beta \frac{w}{w_c}\right)^{0.5} - \left(\beta \frac{w}{w_c}\right) \right] \tag{15} $$

where $p_{max} = 0.5c_u$ with c_u = undrained shear strength; β = scaling factor ($\beta = 1$ in the original expression); and w_c = displacement corresponding to p_{max}. The values of undrained shear strength, c_u, to define p_{max} are determined from the information given in Fig. 7, which is shown in Fig. 10. The values of w_c were computed from the following expression, originally proposed by Randolph and Wroth (1978) and later modified by O'Neill et al. (1982):

$$ w_c = \frac{p_{max}}{2\pi G} \left[0.67 + \log_e \frac{2\overline{G}L(1-v)}{r_0} \right] \tag{16} $$

where L = pile length; $\overline{G}$ = G at the mid-depth of the pile divided by G at the pile tip; and v = Poison's ratio of soil. It was found that the above unit load transfer curve with $\beta = 0.3$ produced the computed static response very close to the response observed in the static load test (Nogami and Paulson, 1984). The initial slopes in the unit load transfer curves (elastic soil stiffnesses) were separately obtained from the initial slope of the load-settlement curve observed in the static load test, in order to correct the curves in the elastic range (Nogami and Paulson, 1984). The above procedure to obtain the elastic stiffness of Winkler subgrade model was previously developed by Nogami and Chen (1984). Assuming these developed curves as backbone curves of a
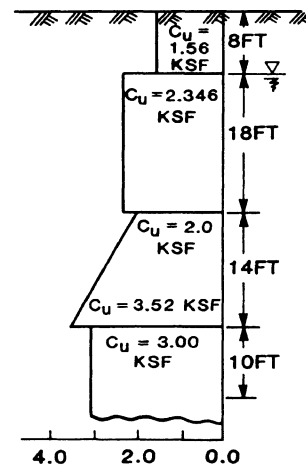

Fig. 10 Undrained shear strength of soil used in computation

hysteresis behavior, input CULT curves are developed: the real parts are backbone curves and the imaginary parts are obtained after constructing the hysteresis loops with these backbone curves and Masing's rule.

405

(c) Prediction of Response and Comparison with Observed Response

Using the above defined input information, pile responses during the vibration test were predicted by the proposed approach. In the computation, the shaft is divided into twenty 2 ft. long segments plus a 3 ft long segment at the bottom.
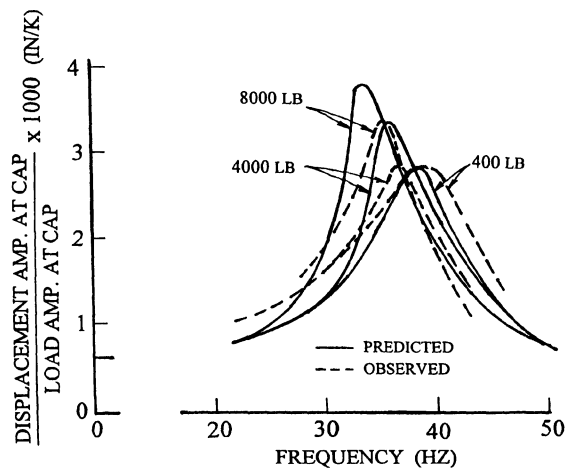

Fig. 11 Variations of displacement amplitude at rigid cap with frequency for various loading amplitudes
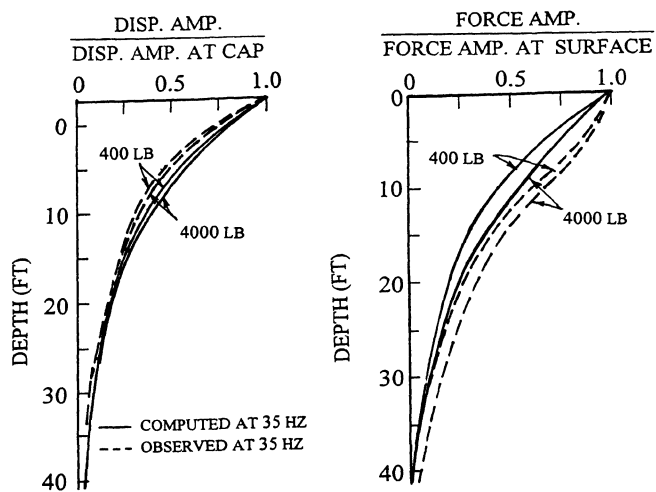

Fig. 12 Distributions of amplitudes of pile displacement and axial force along shaft

The predicted and observed responses are shown in Fig. 11 for variations of displacement amplitude with frequency at the cap. They are also plotted in Figs. 12 and 13 for distributions of displacement and force along the shaft. The peak displacement and its location are reasonably well predicted for the loading amplitude 400 lbs., while the peak displacements are overestimated for higher loading amplitudes. The distribution of the axial force amplitude in the field (Fig. 12) indicates the loose contact between pile and soil within a depth about 7 ft, which might have been caused during pile installation by driving. Although the loose soil-pile contact makes the distribution of the force amplitude in the field somewhat different from the predicted one within

a shallow depth, the predicted force and displacement amplitudes along the shaft appear to be reasonable in general. However, the displacement phase shifts (Fig. 13) are overestimated, particularly for those at 24~36 Hz. When the soil-pile contact is tight, the energy
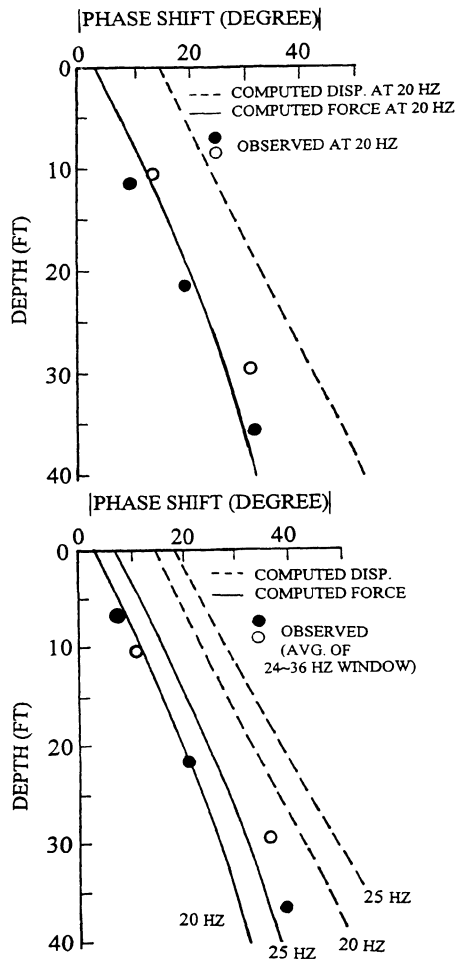

Fig. 13 Distributions of phase shifts of pile displacement and axial force along shaft

dissipates into soil while it travels along the shaft. Thus, the phase shift at a one depth results from the accumulation of the energy loss along the depth from the ground surface through that depth. The analysis did not consider the loose soil-pile contact within a shallow depth. This situation may be corected roughly in the computed phase shift by subtracting the difference, between the phase shifts at 7 ft depth and at the ground surface, from the phase shift at any depth below 7 ft (i.e. shift the curve below 7 ft to the left by the above difference). The corrected phase shifts in this manner are much closer to the observed ones.

CONCLUSIONS

A rational model for a soil-pile interaction is explained for the vertical vibration response analysis of a nonlinear pile foundation. The model parameters are defined by the elastic constants of soil and static CULT cueve. The real part of the CULT curve is a conventional cyclic

406

unit load transfer curve and the imaginary part is related with the hysteresis damping in the static cyclic condition. If the proposed model is defined by the proposed procedure, it can reproduce very well the nonlinear behavior and dynamic behavior mutually coupled and thus the nonlinear dynamic soil-pile interaction force. Both static load tests and vibration tests were conducted on a common pile at the UH site. Pile response during the above vibration tests are predicted by using the proposed model and procedure. Inputs for defining the model parameters are obtained from the static pile load test. The predicted response tends to overestimate the displacement amplitudes for higher loading amplitudes. The displacement phase shift along the pile shaft is particularly overestimated. The discrepancy between the estimated and observed responses appears to be mainly due to the loose soil-pile contact within a shallow depth. In view of the complexity of the conditions, the predicted responses appear to be reasonable.

REFERENCES

Blaney, G.W. and M.W. O'Neill (1986), "Measured Lateral Response of Mass on Single Pile in Clay," J. Geotechnical Engineering Div., ASCE, Vol. 112, No. GT4: 443-457.

Hardin, B.O. and V.P. Drnevich (1972), "Shear Modulus and Damping in Soils," J. Soil Mechanics and Foundation Div., ASCE, Vol. 98, No. SM7: 667-692.

Matlock, H. (1970), "Correlation for the Design of Laterally Loaded Piles in Soft Clay," Preprints, 1970 Offshore Technology Cof., Houston, Texas, April, OTC 1204.

Nogami, T and M. Novak (1980), "Coefficient of Soil Reaction to Pile Vibration," J. Geotechnical Enfineering Div., ASCE, Vol. 106, No. GT5: 565-569.

Nogami, T. and S.K. Paulson (1984), "Winkler Model for Axial Response Analysis of Pile Groups," Symposium on Analysis and Design of Pile Foundations, ASCE National Convention, San Francisco, October 1-5: 287-309.

Nogami, T. and S.L. Chen (1984), "Simplified Approach for Axial Pile Group Response Analysis," J. Geotechnical Engineering Div., ASCE, Vol. 110, No. GT9.

Nogami, T. and K. Konagai (1986), "Dynamic Response of Vertically Loaded Nonlinear Pile Foundations," J. Geotechnical Engineering Div., ASCE, Vol. 113, No. GT2: 147-160.

Nogami, T., J. Otani, K. Konagai and H.L. Chen (1992), "Nonlinear Soil-Pile Interaction for Dynamic Lateral Motion," J. Geotechnical Engineering Div., ASCE, Vol. 118, No. GT1: 89-105.

Novak, M. (1974), "Dynamic Stiffness and Damping of Piles," Canadian Geotechnical J., National Research Council of Canada, Vol. 11, No. 4: 574-598.

Novak, M. T. Nogami and F. Aboul-Ella (1978), "Dynamic Soil Reactions for Plane Strain Case," J. Engineering Mechanics Div., Vol. 104, No. EM4: 950-953.

O'Neill, R.A. Hawkins and L.J. Mahar (1981), "Field Study of Pile Group Action: Final Report, " Report Nos. FHWA/RD-81/002-FHWA/RD 81/008, Federal Highway Administration, U.S. D.O.T., March.

Randolph, M.P. and C.P. Wroth (1978), "Analysis of Deformation of Vertically Loaded Piles," J. Geotechnical Engineering Div., ASCE, Vol. 104, No. GT12: 1465-1488.

Sanchez Salinero, I. (1982), "Static and Dynamic Stiffness of Single Piles," Research Report GR82-31, Dept. of Civil Engineering, The University of Texas, at Austin, Texas.

Vijayvergiya, V.N. (1977), "Load-Movement Characteristics of Piles," Proc. Ports '77, ASCE, Vol. II: 269-286.